

1 **Pain and breathlessness: Salient, somatosensory and similar, but not the same**

2

3 Olivia K. Harrison^{1,2}, Anja Hayen³, Tor D. Wager^{4*} and Kyle T. S. Pattinson^{2*}

4

5 ¹ Translational Neuromodeling Unit, Institute of Biomedical Engineering, University of Zurich and
6 ETH Zurich, Zurich, Switzerland

7 ² Nuffield Department of Clinical Neurosciences, University of Oxford, Oxford, UK

8 ³ School of Psychology & Clinical Language Sciences, University of Reading, Reading, UK

9 ⁴ USA Department of Psychological and Brain Sciences, Dartmouth College, Hanover, USA

10 *Authors contributed equally to this work

11

12 Key words: pain, breathlessness, interoception, threat

13

14

15 Corresponding author:

16 Dr Olivia Harrison (née Faull)

17 Translational Neuromodeling Unit

18 Institute for Biomedical Engineering

19 University of Zurich and ETH Zurich

20 Zurich, Switzerland

21 Email: faull@biomed.ee.ethz.ch

22 **Abstract**

23 Quantifying pain currently relies upon subjective self-report. Alongside the inherent variability
24 embedded within these metrics, added complications include the influence of ambiguous or prolonged
25 noxious inputs, or in situations when communication may be compromised. As such, there is continued
26 interest in the development of brain biomarkers of pain, such as in the form of neural ‘signatures’ of
27 brain activity. However, issues pertaining to pain-related specificity remain, and by understanding the
28 current limits of these signatures we can both progress their development and investigate the
29 potentially generalizable properties of pain to other salient and/or somatomotor tasks. Here, we utilized
30 two independent datasets to test one of the established Neural Pain Signatures (the NPS (Wager et al.
31 2013)). In Study 1, brain activity was measured using functional magnetic resonance imaging (fMRI)
32 in 40 healthy subjects during experimentally induced breathlessness, conditioned anticipation of
33 breathlessness and a simple finger opposition task. In Study 2, brain activity was again measured
34 during anticipation and breathlessness in 19 healthy subjects, as well as a modulation with the opioid
35 remifentanil. We were able to identify significant NPS-related brain activity during anticipation and
36 perception of breathlessness, as well as during finger opposition using the global NPS. Furthermore,
37 localised NPS responses were found in early somatomotor regions, bilateral insula and dorsal anterior
38 cingulate for breathlessness and finger opposition. In contrast, no conditions were able to activate the
39 local signature in the dorsal posterior insula - thought to be critical for pain perception. These results
40 provide properties of the present boundaries of the NPS, and offer insight into the overlap between
41 breathlessness and somatomotor conditions with pain.

42 **Introduction**

43

44 Whilst perceptions of pain are often identified and assessed through subjective self-report, these
45 experiences are influenced by higher cognitive functions such as attention (Wiech et al. 2008) and
46 expectation (Atlas & Wager 2012). Furthermore, pain perception can be altered with prolonged
47 noxious inputs, and are potentially difficult to quantify in infants, in those who have cognitive
48 impairment, or those who are minimally conscious (Wager et al. 2013). Therefore, the quest has begun
49 for biological ‘readouts’ related to pain in the brain, with the hope of allowing us to assess pain within
50 an individual using non-invasive neuroimaging measures (Wager et al. 2013; Woo, Schmidt, et al.
51 2017). These tools are designed to identify pain across experiments and laboratories, and eventually
52 lead to use in those who cannot accurately express pain for themselves.

53 Here we focus on the Neurologic Pain Signature (NPS), an established pain-related brain
54 measure. An advantage of this measure is that it has been widely tested—on over 40 unique participant
55 cohorts to date—for sensitivity and specificity to pain, generalizability across populations and evoked
56 pain types, and other properties (for reviews, see (Woo, Chang, et al. 2017; Kragel et al. 2018)). The
57 NPS is a distributed pattern of activity across brain regions, including the major targets of ascending
58 nociceptive pathways (dorsal posterior insula, ventrolateral and medial thalamus, mid- and anterior
59 insula, anterior midcingulate, amygdala, periaqueductal gray, hypothalamus). It can be applied to
60 individual-person level data across studies (Wager et al. 2013), yielding an objective brain measure
61 (Woo & Wager 2016)1. Applying the NPS entails calculating a weighted average across voxels for a
62 test functional brain image (i.e., the dot product) or another pattern similarity metric. Pattern weights
63 limited to individual regions can also be used to obtain local pattern responses (Woo et al. 2014).

64 This approach is part of a major trend in neuroimaging research using pattern information to
65 assess pain (Rosa & Seymour 2014; Mano et al. 2018; van der Miesen et al. 2019; Ung et al. 2012;
66 Marquand et al. 2010) and other cognitive and affective processes. Multivariate brain models integrate

67 brain information into a single optimized prediction, and test predictions on new, independent
68 individuals, providing unbiased estimates of effect size (Reddan et al. 2017) and capturing information
69 across multiple spatial scales (Miyawaki et al. 2008; Hackmack et al. 2012; Haynes 2015; Lindquist
70 et al. 2017). NPS responses have also been found to correlate with the intensity of variations in evoked
71 experimental pain in individuals across multiple studies (Lindquist et al. 2017; Woo, Schmidt, et al.
72 2017). In one analysis across 6 studies (N = 180), NPS responses were positively correlated with trial-
73 by-trial pain reports in 93% of individual participants (Lindquist et al. 2017). The NPS has also been
74 shown to demonstrate some specificity towards somatic pain: It does not respond to non-noxious warm
75 stimuli (Wager et al. 2013), threat cues (Wager et al. 2013; Krishnan et al. 2016; Ma et al. 2016), social
76 rejection-related stimuli (Wager et al. 2013), observed pain (Krishnan et al. 2016), or aversive images
77 (Chang et al. 2015), although many of these conditions are affective, salient, and activate many of the
78 same gross anatomical regions as somatic pain. Therefore, the NPS is not a complete model for all
79 types of and influences on pain (Woo, Schmidt, et al. 2017), but rather appears to track pain of
80 nociceptive origin (including thermal, mechanical, laser, visceral, and electrical; (Krishnan et al. 2016;
81 Woo & Wager 2016; López-Solà et al. 2017; Zunhammer et al. 2018)) in a fashion that is relatively
82 insensitive to cognitive input. It does not respond to social ‘pain’ (Woo et al. 2014; Krishnan et al.
83 2016), and it is not strongly influenced by placebo treatment (Zunhammer et al. 2018), cognitive
84 regulation (Woo et al. 2015), reward (Becker et al. 2017), knowledge about drug-delivery context
85 (Wager et al. 2013; Zunhammer et al. 2018), or perceived control (Bräscher et al. 2016). On the other
86 hand, the NPS does show significant responses to remifentanil, citalopram, spinal manipulation (in
87 chronic neck pain sufferers), and some types of psychosocial/behavioral manipulations, showing
88 promise as a pharmacodynamic biomarker. These findings underscore the idea that the NPS and other
89 brain measures do not “measure pain” (a subjective experience), but rather measure specific
90 neurophysiological processes linked to pain construction.

91 However, whilst early results have proven promising when delineating pain from other
92 emotion-based stimuli, these measures have not typically been tested against predominantly
93 somatosensory aversive stimuli. One ideal test case might be the frightening perception of
94 breathlessness; a multi-dimensional symptom that causes major suffering across a broad range of
95 individuals (Marlow et al. 2019; Hayen et al. 2013; Herigstad et al. 2011). In fact, the definition of
96 breathlessness (or ‘dyspnea’) from the American Thoracic Society draws many comparisons that
97 closely parallel perceptions of pain (Parshall et al. 2012), and previous work has noted many
98 similarities between brain networks associated with both breathlessness and pain (Leupoldt et al.
99 2009). However, whether this broad correspondence is represented within more highly localized pain
100 signatures, and what this means for our understanding of these vastly different perceptions, is not yet
101 known. Furthermore, isolated somatomotor activity has also yet to be exclusively tested against these
102 pain signatures, many of which load heavily on somatomotor networks within the brain (Cauda et al.
103 2012).

104 Here, we aimed to test the specificity of the Neural Pain Signature (NPS, (Wager et al. 2013))
105 using salient and somatomotor tasks. We employed two datasets that induced both the anticipation and
106 perception of breathlessness (Study 1 – collected at 7 Tesla in 40 healthy subjects (Faull & Pattinson
107 2017); and Study 2 – collected at 3 Tesla in 19 healthy subjects (Hayen et al. 2017)), and a simple
108 somatomotor task of finger opposition (Study 1). We then investigated local patterns of pain-related
109 activity from the regional NPS responses, allowing us to disentangle where the major similarities or
110 differences may exist between these conditions. Additionally, we explored the effect of opioid
111 administration (Study 2) to test the potential modulation of the global and regional NPS responses to
112 both the anticipation and perception of breathlessness. We aimed to find the boundary conditions for
113 the NPS to both understand existing limitations and generalizable properties as a biomarker for pain,
114 support its refinement towards greater pain specificity, and investigate the potential neural similarities
115 and differences between pain and breathlessness.

116

117

118 **Methods**

119

120 *Testing data sets*

121 To test the current limitations of the NPS, data from previously published work was utilized in these
122 analyses (Faull & Pattinson 2017; Hayen et al. 2017) (please see previous publications for a full
123 description of the study methods, scanning protocols and univariate analyses). Briefly, the first dataset
124 was acquired at 7 Tesla (Faull & Pattinson 2017), and employed one level of breathlessness (induced
125 by inspiratory resistive loading) during fMRI, with preceding anticipation periods cued by conditioned
126 shapes presented on the screen. Control tasks of no anticipation or breathlessness (cued via the
127 presentation of a conditioned shape that was never paired with breathlessness) and finger opposition
128 (cued by the word 'tap' presented on the screen) were also collected. Each condition was presented 14
129 times in a pseudo-randomised order. The contrasts of interest that were analysed against the NPS for
130 this study were anticipation > no breathlessness cue ('Anticipation' contrast), breathlessness > no
131 breathlessness ('Breathlessness' contrast), and finger opposition > baseline ('Finger opposition'
132 contrast).

133 The second dataset was acquired at 3 Tesla (Hayen et al. 2017), and employed two levels of
134 breathlessness (mild and strong, also induced with inspiratory resistive loading) with conditioned
135 anticipation periods, and a cued control condition of no anticipation or breathlessness (as above). Four
136 repeats of each of the paired anticipation and breathlessness cues were presented, and eight repeats of
137 the unloaded condition were performed (pseudo-randomised order). This study involved two scans,
138 with either a controlled infusion of the opioid remifentanil (0.7 ng/ml target) or saline placebo (single-
139 blind, counterbalanced order). For this analysis, we have not considered the anticipation and perception
140 of mild breathlessness, to remain consistent and attempt to replicate any results found in Study 1. The

141 contrasts of interest that were analysed against the NPS here were anticipation of strong breathlessness
142 > no breathlessness cue in the saline condition ('Anticipation' contrast), strong breathlessness > no
143 breathlessness in the saline condition ('Breathlessness' contrast), anticipation of strong breathlessness
144 > no breathlessness cue in the remifentanil condition ('Remi Anticipation' contrast), and strong
145 breathlessness > no breathlessness in the remifentanil condition ('Remi Breathlessness' contrast). The
146 difference between saline and remifentanil conditions were also compared for both anticipation and
147 breathlessness contrasts.

148

149 *NPS analyses*

150 For each contrast in each study, we calculated the overall NPS response as specified by Wager and
151 colleagues (Wager et al. 2013). This entailed taking the dot product of the NPS weight map and each
152 test contrast image from each individual participant, calculating a weighted average over each test
153 image, where the NPS map specifies the weights. It reduces each contrast image to a single number,
154 the 'NPS response', which is the predicted pain intensity based on the model. We tested whether the
155 NPS responses were significantly different from zero using standard t-tests. This is mathematically
156 equivalent to conducting paired t-tests on within-person contrasts, treating participant as a random
157 effect. We also applied the local NPS patterns from nociceptive target regions with predominantly
158 positive weights ('NPS Positive' subregions) and regions with negative weights ('NPS Negative'
159 subregions), as defined in (López-Solà et al. 2017) and (Krishnan et al. 2016). We use a standard
160 threshold of $p < 0.05$ for statistical significance in these a priori tests (one star in figures), and also
161 note tests that are significant at $p < 0.01$ (two stars) and $q < 0.05$ False Discovery Rate corrected (three
162 stars). Finally, we tested whether NPS responses were related to sedation levels and the order in which
163 conditions were administered.

164

165 **Results**

166 Anticipation of breathlessness, breathlessness perception and finger opposition all significantly
167 activated the overall NPS (Table 1 and Figure 1), and the findings for anticipation and breathlessness
168 were able to be replicated in two independent datasets. The administration of remifentanil in Study 2
169 did not alter the NPS response to anticipation of breathlessness, and while it appeared to reduce the
170 response to breathlessness itself, this did not reach statistical significance (Table 1).

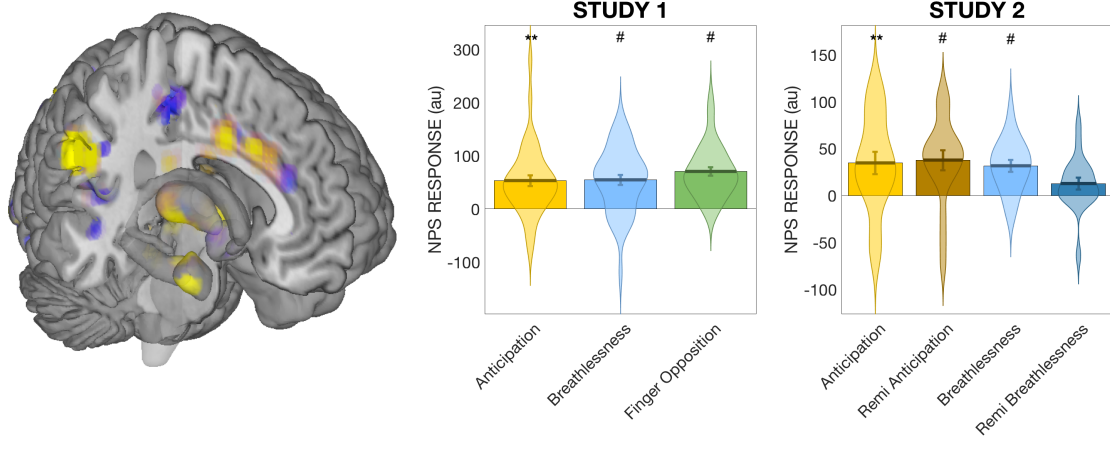
171

172 *Table 1.* NPS responses and statistics for the contrasts of interest in each study. Study 1 was conducted
173 at 7 Tesla with 40 participants and 14 stimulus repeats, while Study 2 was collected at 3 Tesla with 19
174 participants and 4 stimulus repeats.

STUDY	CONTRAST	NPS RESPONSE	STD ERROR	T-STAT	P-VALUE	COHEN'S D
1	Anticipation	53.24	10.39	5.12	<0.01	0.81
	Breathlessness	54.62	9.55	5.72	<0.01	0.90
	Finger opposition	70.47	7.72	9.13	<0.01	1.44
2	Anticipation (S)	34.80	11.80	2.95	<0.01	0.68
	Breathlessness (S)	37.81	10.60	3.57	<0.01	0.82
	Anticipation (R)	31.72	6.30	5.04	<0.01	1.16
	Breathlessness (R)	12.84	6.47	1.98	0.06	0.46
	S>R Anticipation	-3.01	12.37	-0.24	0.81	-0.06
	S>R Breathlessness	18.88	9.30	2.03	0.06	0.47

175

176



177

178 *Figure 1.* Overall NPS activity in the contrasts of interest for the two datasets. Left: Three-dimensional
179 representation of some of the core regions of the NPS. ** Significantly different from zero at $p < 0.01$
180 (most satisfy $p < 0.001$); # Significantly different from zero at $q < 0.05$ (FDR corrected).

181

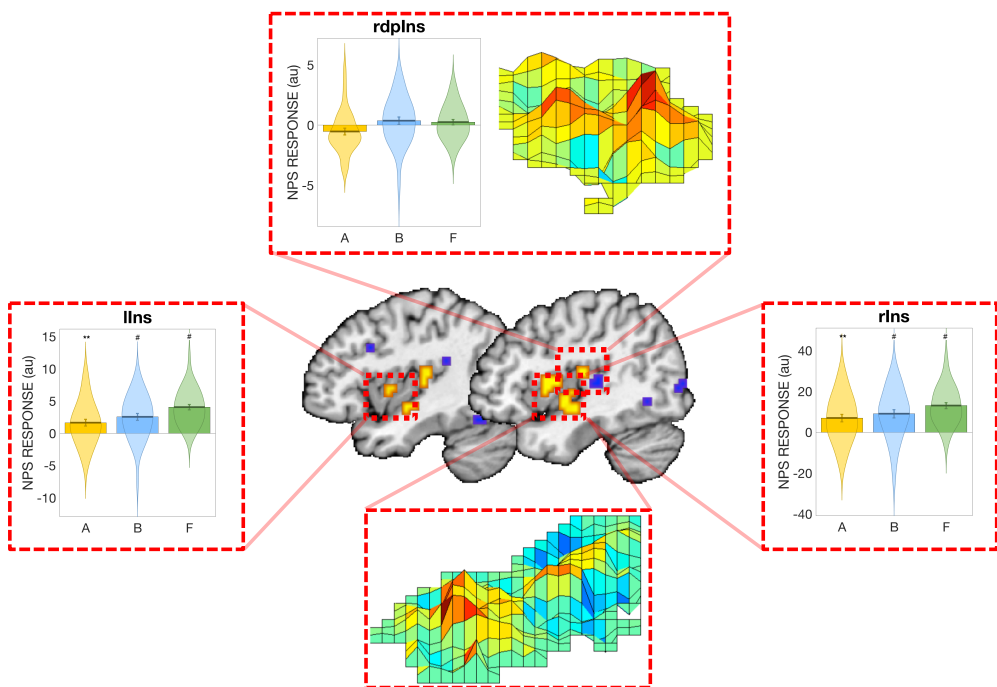
182

183 *Study 1 regional NPS results*

184 Within the NPS subregions, the anticipation contrast produced significant responses in the positive
185 NPS regions of the bilateral insula, and significant responses in the negative NPS regions of the
186 bilateral lateral occipital cortex and right inferior parietal lobule (Figures 2 and 3; Supplementary Table
187 1). During breathlessness, significant responses were observed in the positive NPS regions of the
188 bilateral insula, right thalamus, right secondary sensory cortex, dorsal anterior cingulate cortex and
189 vermis, and significant responses in the negative NPS region of the right inferior parietal lobule
190 (Figures 2 and 3; Supplementary Table 1). Consistent with the breathlessness contrast, finger
191 opposition also produced significant responses in the positive NPS regions of the bilateral insula, right
192 thalamus, right secondary sensory cortex, dorsal anterior cingulate cortex and vermis, plus additional
193 activity in the right primary visual cortex. In the negative NPS regions, finger opposition activated the
194 lateral occipital cortex and right posterior lateral occipital cortex (Supplementary Table 1). No
195 contrasts produced significant activity in the right dorsal posterior insula subregion of the NPS (Figure

196 2). Full statistical reports and visualisations of the raw condition-related activity are provided in the
197 supplementary material.

198



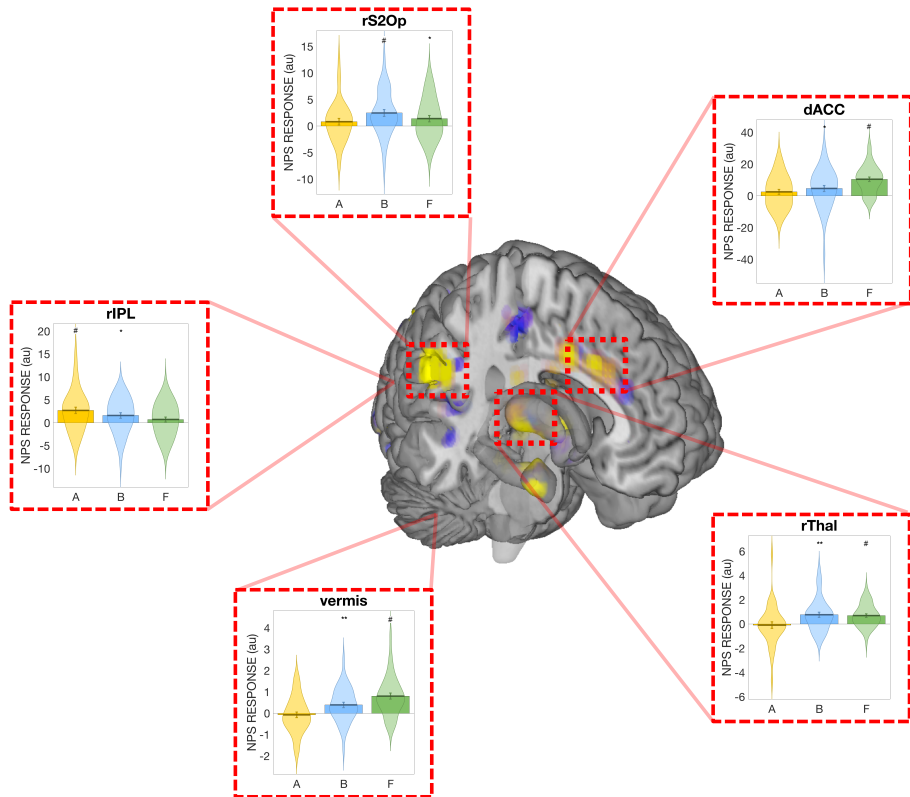
199

200 *Figure 2.* Regional NPS activity in the insula for the anticipation, breathlessness and finger opposition
201 contrasts from Study 1. Robust statistical activity is observed in the bilateral insula (labelled lIns and
202 rIns) for all three conditions, while no significant activity is observed in the right dorsal posterior insula
203 (rdpIns). Abbreviations: A, Anticipation contrast; B, Breathlessness contrast; F, Finger opposition
204 contrast. ** Significantly different from zero at $p < 0.01$; # Significantly different from zero at $q <$
205 0.05 (FDR corrected).

206

207

208



209

210 *Figure 3.* Regional NPS activity subregions of the NPS for the anticipation, breathlessness and finger
 211 opposition contrasts from Study 1. Significant NPS activation is observed in the dorsal anterior
 212 cingulate cortex (dACC), right thalamus (rThal), right secondary somatosensory cortex / operculum
 213 (rS2Op) and vermis for both breathlessness and finger opposition, and in the right inferior parietal
 214 lobule (rIPL) for both anticipation and breathlessness. For a full list of regions please see
 215 Supplementary Table 1. Abbreviations: A, Anticipation contrast; B, Breathlessness contrast; F, Finger
 216 opposition contrast. * Significantly different from zero at $p < 0.05$; ** Significantly different from zero
 217 at $p < 0.01$; # Significantly different from zero at $q < 0.05$ (FDR corrected).

218

219

220 *Study 2 regional NPS results*

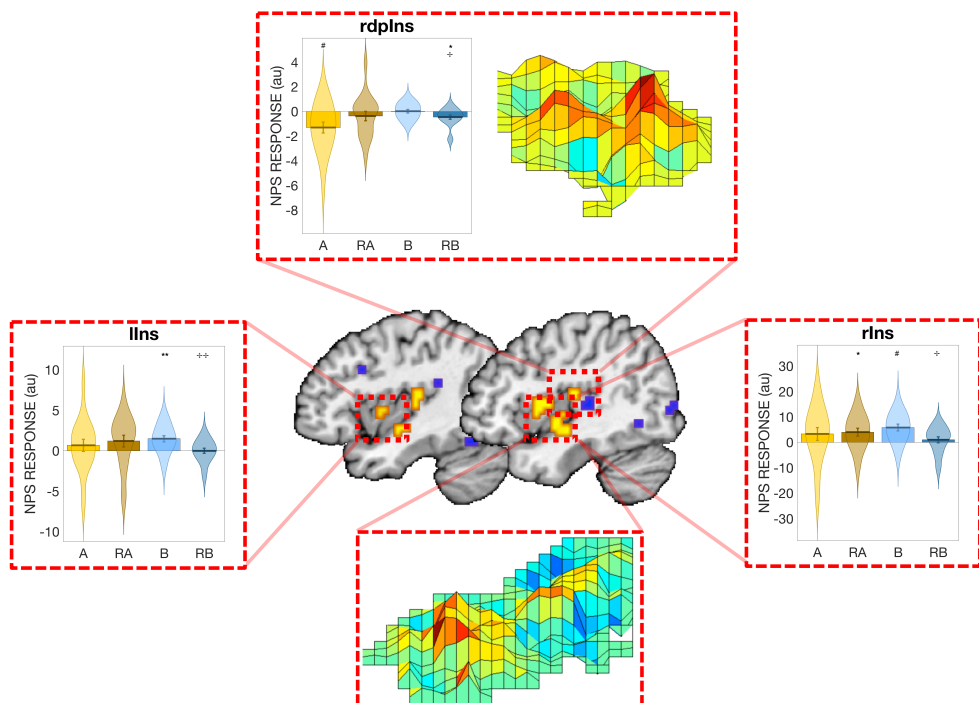
221 Within the positive NPS subregions in Study 2, the anticipation (saline) contrast produced a significant
 222 response in the right primary visual cortex, with a negative response in the right dorsal posterior insula

223 (Figures 4 and 5; Supplementary Table 2). No significant responses were found in the negative NPS
224 subregions. The administration of remifentanil did not significantly modulate any of the NPS-related
225 subregion activity during anticipation, although the right insula (positive region) and right posterior
226 lateral occipital cortex and left superior temporal sulcus (negative regions) all additionally produced
227 significant results (Figures 4 and 5; Supplementary Table 2).

228 During breathlessness, the positive NPS regions of bilateral insula, right thalamus, right
229 secondary sensory cortex and dorsal anterior cingulate cortex produced significant NPS-related
230 activity, while the negative NPS subregion of the pregenual anterior cingulate cortex was also
231 significant (Figures 4 and 5; Supplementary Table 2). The administration of remifentanil significantly
232 decreased the NPS-related activity in all saline significant regions except the pregenual anterior
233 cingulate cortex, and additionally produced a significant decrease in the right dorsal posterior insula
234 (Figures 4 and 5; Supplementary Table 2).

235

236

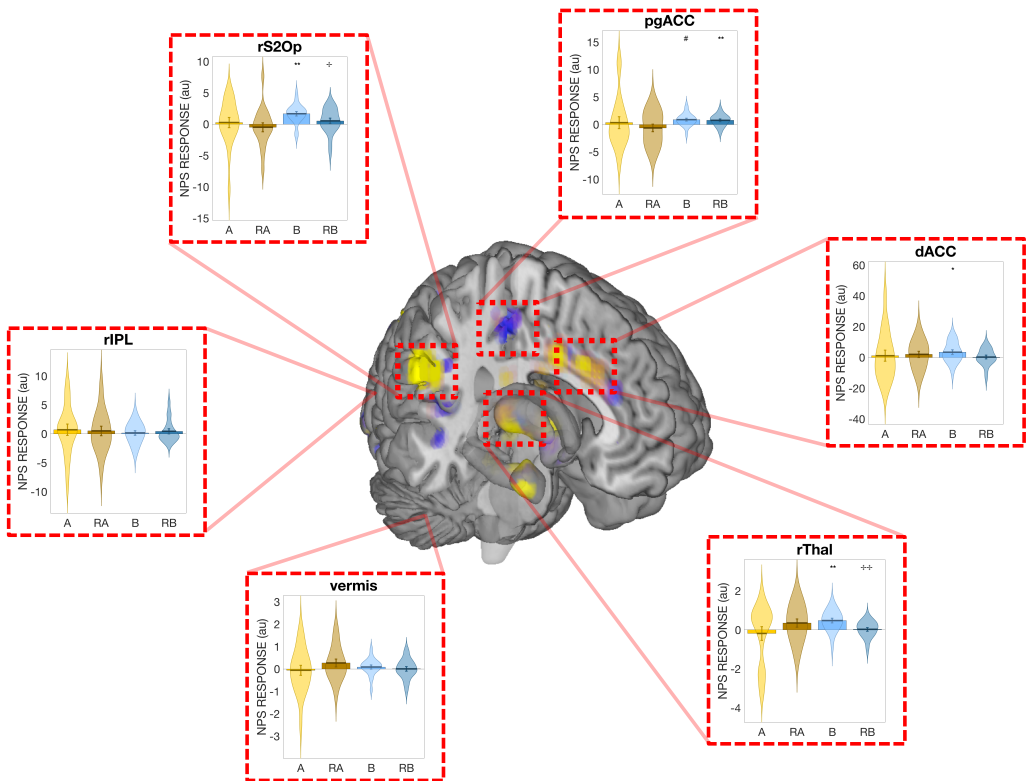


237

238 *Figure 4.* Regional NPS activity in the insula for the anticipation and breathlessness contrasts during
239 both saline and remifentanil administration from Study 2. Robust, positive statistically significant
240 NPS-related activity is only observed in the bilateral insula (labelled lIns and rIns) for the
241 breathlessness condition, which is significantly modulated by the administration of the opioid
242 remifentanil. NPS-related activity in the right dorsal posterior insula (rdpIns) is significantly decreased
243 during saline anticipation. Abbreviations: A, Anticipation contrast (saline); RA, Remifentanil
244 anticipation contrast; B, Breathlessness contrast (saline); RB, Remifentanil breathlessness contrast. **
245 Significantly different from zero at $p < 0.01$; # Significantly different from zero at $q < 0.05$ (FDR
246 corrected); ⁺⁺ Significantly modulated by remifentanil at $p < 0.05$.

247

|248



251 *Figure 5.* Regional NPS activity subregions of the NPS for the anticipation and breathlessness
 252 contrasts during both saline and remifentanil administration from Study 2. Significant NPS activation
 253 is observed in the dorsal and pregenual anterior cingulate cortex (dACC and pgACC), right thalamus
 254 (rThal) and right secondary somatosensory cortex / operculum (rS2Op) for breathlessness, with the
 255 NPS-related activity in the right thalamus and rS2Op significantly modulated by the administration of
 256 the opioid remifentanil. For a full list of regions please see Supplementary Table 2. Abbreviations: A,
 257 Anticipation contrast (saline); RA, Remifentanil anticipation contrast; B, Breathlessness contrast
 258 (saline); RB, Remifentanil breathlessness contrast. * Significantly different from zero at $p < 0.05$; **
 259 Significantly different from zero at $p < 0.01$; # Significantly different from zero at $q < 0.05$ (FDR
 260 corrected); + Significantly modulated by remifentanil with $p < 0.05$; ++ Significantly modulated by
 261 remifentanil at $p < 0.01$.

263

264 **Discussion**

265

266 *Main findings*

267 Utilising two independent datasets, we have demonstrated that both the anticipation and perception of
268 breathlessness robustly evoked significant activity in an established pain signature (NPS (Wager et al.
269 2013)), and this NPS-related activity during breathlessness was able to be modulated by the infusion
270 of the short-acting opioid remifentanil (Study 2). Furthermore, a somatomotor finger opposition task
271 was also able to evoke significant activity within the NPS. When specific subregions of the NPS were
272 examined, pain-related patterns in the anterior cingulate cortex, bilateral insula, thalamus, secondary
273 sensory cortex and vermis responded to both breathlessness and finger opposition, with all
274 breathlessness results (except the vermis) replicated in an independent study at 3 Tesla. Additionally,
275 the insula, thalamus and secondary somatosensory cortex (S2) were all modulated by the
276 administration of the opioid remifentanil. The activity in these areas may thus provide a general
277 substrate for motivated action within the pain response. In contrast, no conditions positively activated
278 the local NPS pattern in the dorsal posterior insula, an area though to be a critical area for pain
279 perception. Therefore, these results provide new information on the boundary conditions for NPS
280 activation, where a non-zero NPS value is not sufficient to discriminate pain from breathlessness,
281 anticipation of breathlessness, and basic sensorimotor activity. These findings contrast with a number
282 of previous studies that have not found anticipatory activity during anticipated pain (Krishnan et al.
283 2016; López-Solà et al. 2019). The findings thus suggest that new classifiers, perhaps based on
284 conjunctions of local pattern responses in specific areas, may be required to achieve further specificity.
285 In this regard, the dorsal posterior insula (dpIns) may be a key region, as dpIns (and local NPS pattern
286 in this region) is routinely activated during somatic pain (Geuter et al. 2020), but does not appear to
287 respond to any of the challenges studied here.

289 *Implications for the understanding of breathlessness*

290 Our findings may also provide insight into the similarities and differences underlying these
291 somatosensory (and often salient) conditions. Current theories regarding the mechanisms and potential
292 treatments for chronic breathlessness often draw heavily on pain models (Parshall et al. 2012; Leupoldt
293 et al. 2009; Lansing et al. 2009), which is understandable considering that they share some
294 phenomenological characteristics. However, with the search for individualised neuro-markers and
295 brain-based treatments for breathlessness becoming an increasing topic of interest (Marlow et al. 2019;
296 Herigstad et al. 2017), it is imperative to attempt to understand what is specific for breathlessness
297 within brain activity and connectivity patterns, rather than over-rely on models created from other
298 conditions.

300 *Specificity of neural pain signatures*

301 These results help us to understand and explore the current boundaries of an established neural pain
302 signature. While NPS-related activity was significantly activated by non-pain conditions, qualitative
303 pattern differences existed within the regional responses across specific areas. Notably, while
304 sensorimotor areas and the bilateral insula were repeatedly activated by non-painful but somatosensory
305 tasks, the dorsal posterior insula was not positively activated by any of the conditions tested here. The
306 dorsal posterior insula has been frequently implicated as having a critical role in pain perception
307 (Henderson et al. 2010; Brooks et al. 2005; Singer et al. 2004; Ito 1998; Craig 2013; Segerdahl et al.
308 2015), and may be an essential area in differentiating pain from other salient symptoms. Previous work
309 in both animals (Ito 1998; Craig 2013) and humans (Segerdahl et al. 2015) has determined a subregion
310 of the dorsal posterior insula to be a cortical representation of afferent nociceptive stimuli, and thus it
311 could be considered as an important primary sensory junction for ascending peripheral pain stimuli.

312 Therefore, it is possible that localized patterns of activity in this specific area of the brain may prove
313 more informative for specific determination of painful from non-painful stimuli.

314

315 *Neural signatures of motivated actions*

316 While the brain is thought to contain primary cortices dedicated to specific sensory experiences such
317 as vision, audition and touch (Liang et al. 2013; Kwong et al. 1992; Noesselt et al. 2007; Goel et al.
318 2006), processing of sensory signals does not stop at these junctures. We must de-code these sensory
319 inputs – together with our expectations of the world around us (Seth 2013; Stephan et al. 2016; Van
320 den Bergh et al. 2017; Feldman Barrett & Simmons 2015; Marlow et al. 2019) – to determine what
321 they mean for elements of our health and happiness, and the potential necessity for any further action.

322 Thus, processing these multiple dimensions of perceptual information requires higher cortical
323 involvement and communications beyond primary sensory cortices. While multivariate, brain-wide
324 signatures such as the NPS have been developed to specifically determine the pattern of activity
325 associated with perceptions of somatosensory pain (Wager et al. 2013; Woo, Schmidt, et al. 2017),
326 these complex, salient experiences may not be easily discernable from other threatening perceptions
327 or even simply motivated behaviors in some cases.

328 Here, we have shown that not only does breathlessness evoke similar patterns of brain activity
329 to that of painful stimuli, but also that anticipating breathlessness and even a simple finger opposition
330 task can both significantly activate the NPS. While the lived experience of these conditions informs
331 us that they are usually easily separable and distinct experiences, they must share common threads
332 within both their nature and activated brain networks. In essence, they all involve the translation of
333 sensory signals to desired motivated behaviors: to avoid the painful stimulus, to overcome the
334 inspiratory resistance (or to prepare for this during an anticipatory period), and to conduct finger
335 opposition movements. When we consider the regional NPS responses to these conditions within the
336 brain, we observe statistical similarities between pain, breathlessness and finger opposition in the

337 thalamus, secondary sensory cortex, bilateral insula and dorsal anterior cingulate cortex. These areas
338 are indeed associated with early sensory processing (thalamus and secondary sensory cortex) (Craig
339 et al. 1994; Ohara & Lenz 2003; Ploner et al. 1999), representations of bodily state (insula) (Singer et
340 al. 2009; Craig 2002; Craig 2009; Craig 2003) and context-specific behaviors towards directed goals
341 (dorsal anterior cingulate) (Holroyd & Yeung 2012), and thus may provide a representative network
342 of sensation-motivated behaviors. However, as anticipation of breathlessness can also induce
343 significant activity in the NPS, it does not appear that the presence of sensory information flow from
344 the periphery is a necessity to activate this blueprint of ‘motivated action’. Rather, the preparatory,
345 future-oriented intent for motivated action may be powerful enough to elicit an NPS-related brain
346 response. Notably, many other salient, motivationally relevant affective conditions have failed to
347 produce NPS activation in previous studies. One possibility for the discrepancy between these studies
348 and the present ones is that many previous comparison conditions involved emotional responses, which
349 appear to engage substantially different brain systems overall from those engaged by pain. Perhaps
350 finger opposition, counterintuitively, produces activity patterns more similar to the NPS because it
351 engages basic motivational, attentional and action processes without the additional different systems
352 engaged during emotion.

353 There is one important additional caveat. It is unclear from the present results alone whether
354 the degree of activation to breathlessness and its anticipation is comparable to that elicited by somatic
355 pain (Wager et al. 2013), where a quantitative threshold was needed to separate pain from non-painful
356 stimuli, as emotion and non-painful warmth produced relative NPS response differences in the sub-
357 pain-threshold range. Therefore, we cannot know for sure whether the NPS responses observed here
358 are quantitatively strong enough to be classified as “pain” by the original model. Because BOLD signal
359 is not measured in absolute units it remains a challenge to be addressed in the future to compare NPS
360 responses (and other metrics) quantitatively across studies. To further complicate matters, the added
361 signal and statistical power provided across field strengths (such as using 7 Tesla) or between different

362 conditions (such as pain, breathlessness and finger opposition) may overwhelm prescribed magnitude
363 ‘thresholds’ for NPS activity, and thus also need to be considered. While further experimentation
364 including pain, breathing and sensorimotor tasks within one session at the same field strength may
365 shed light on these magnitude differences, the current results do appear to inform us that a simple
366 ‘significant’ activation of these signatures cannot constitute ‘pain’ alone. Moreover, the fact that we
367 observed some NPS activity here in response to non-somatic pain conditions motivates the
368 development and validation of other types of models.

369

370 *Conclusions and future directions*

371 So, what do these results mean for the NPS? And for our understanding of breathlessness? Are we
372 chasing the impossible, where a pattern of whole-brain activity can identify pain and pain alone in an
373 individual? And what would the perception of pain become, if the component comprising motivated
374 behavior were removed? We could strive for finer resolutions and better pattern recognition
375 algorithms, with the hope that this specificity exists underneath the noise of functional neuroimaging.
376 Or, with the inherent spatial constraints imposed upon us, and the diversity of brains among us (Gordon
377 et al. 2017), it may be more fruitful to move away from a modular view of the (non-invasively
378 accessible) macro-scale brain, and consider that the existence of a highly specific ‘pain activity
379 network’ may not be achievable given both the importance of cognitive context in shaping pain and
380 the current functional neuroimaging tools (Atlas & Wager 2012; Wiech et al. 2008). That is, somatic
381 conditions such as breathlessness and finger opposition, and even types of anticipatory threat that are
382 sufficiently intense and strongly referred to the body may activate (what has been thought of as)
383 somatic ‘pain’ systems.

384 Alternatively, we could narrow our initial search to more primary sensory cortices that have
385 repeatedly been associated specifically with pain, such as the dorsal posterior insula (Henderson et al.
386 2010; Brooks et al. 2005; Singer et al. 2004; Ito 1998; Craig 2013; Segerdahl et al. 2015). These

387 localized patterns could then be combined using rule-based classifiers or combined with brain-wide
388 indicators, and possibly extended and combined with more intricate measures of regional connectivity
389 patterns within dynamic functional networks (Woo et al. 2015). Thus, the present results, alongside
390 animal neuroscience studies showing high specificity of neural populations for particular subtypes of
391 pain and body locations, offer substantial promise for developing pain-specific and breathlessness-
392 specific signature patterns. Understanding both brain activity and connectivity may also provide clues
393 as to the flow of information between primary sensory cortices and higher cognitive and limbic
394 structures, and may thus offer the required specificity to help us identify pain in those who cannot
395 express it for themselves.

396

397

398 **Conflict of interest statement**

399 The authors have no conflicts of interest to declare.

400

401

402 **Acknowledgements**

403 Olivia Harrison (née Faull) is a Marie Skłodowska-Curie Postdoctoral Fellow, supported by the
404 European Union's Horizon 2020 research and innovation programme under the Grant Agreement No
405 793580. This work was supported in part by NIH grants R01DA035484, 2R01MH076136 and
406 R01DA027794 (TDW). Kyle Pattinson was supported by the JABBS Foundation, the Dunhill Medical
407 Trust, and the NIHR Biomedical Research Centre based at Oxford University Hospitals NHS Trust
408 and The University of Oxford. This article is based upon work funded by a Medical Research Council
409 Clinician Scientist Fellowship (grant number G0802826) awarded to K.T.S.P.

410 **References**

411 Atlas, L.Y. & Wager, T.D., 2012. How expectations shape pain. *Neuroscience Letters*, 520(2),
412 pp.140–148.

413 Becker, S. et al., 2017. Orbitofrontal cortex mediates pain inhibition by monetary reward. *Social*
414 *Cognitive and Affective Neuroscience*, 12(4), pp.651–661.

415 Bräscher, A.-K. et al., 2016. Different Brain Circuitries Mediating Controllable and Uncontrollable
416 Pain. *The Journal of neuroscience : the official journal of the Society for Neuroscience*, 36(18),
417 pp.5013–5025.

418 Brooks, J.C.W. et al., 2005. Somatotopic organisation of the human insula to painful heat studied
419 with high resolution functional imaging. *Neuroimage*, 27(1), pp.201–209.

420 Cauda, F. et al., 2012. Shared “Core” Areas between the Pain and Other Task-Related Networks D.
421 R. Chialvo, ed. *PLOS ONE*, 7(8), pp.e41929–10.

422 Chang, L.J. et al., 2015. A Sensitive and Specific Neural Signature for Picture-Induced Negative
423 Affect R. Adolphs, ed. *PLoS Biology*, 13(6), pp.e1002180–28.

424 Craig, A.D., 2009. How do you feel---now? the anterior insula and human awareness. *Nature*
425 *Reviews Neuroscience*. Available at: <http://psycnet.apa.org/psycinfo/2009-00363-005>.

426 Craig, A.D., 2002. How do you feel? Interoception: the sense of the physiological condition of the
427 body. *Nature Reviews Neuroscience*, 3(8), pp.655–666.

428 Craig, A.D., 2003. Interoception: the sense of the physiological condition of the body. *Current*
429 *opinion in neurobiology*, 13(4), pp.500–505.

430 Craig, A.D., 2013. Topographically organized projection to posterior insular cortex from the
431 posterior portion of the ventral medial nucleus in the long-tailed macaque monkey. *The Journal*
432 *of comparative neurology*, 522(1), pp.36–63.

433 Craig, A.D. et al., 1994. A thalamic nucleus specific for pain and temperature sensation. *Nature*,
434 372(6508), pp.770–773.

435 Faull, O.K. & Pattinson, K.T., 2017. The cortical connectivity of the periaqueductal gray and the
436 conditioned response to the threat of breathlessness. *eLife*, 6, p.95. Available at:
437 <http://elifesciences.org/lookup/doi/10.7554/eLife.21749>.

438 Feldman Barrett, L. & Simmons, W.K., 2015. Interoceptive predictions in the brain. *Nature Reviews*
439 *Neuroscience*, 16(7), pp.419–429.

440 Geuter, S. et al., 2020. Multiple Brain Networks Mediating Stimulus–Pain Relationships in Humans.
441 *Cerebral Cortex*, pp.322–16.

442 Goel, A. et al., 2006. Cross-modal regulation of synaptic AMPA receptors in primary sensory
443 cortices by visual experience. *Nature Neuroscience*, 9(8), pp.1001–1003.

444 Gordon, E.M. et al., 2017. Precision Functional Mapping of Individual Human Brains. *Neuron*,
445 95(4), pp.791–807.

446 Hackmack, K. et al., 2012. Multi-scale classification of disease using structural MRI and wavelet
447 transform. *Neuroimage*, 62(1), pp.48–58.

448 Hayen, A. et al., 2017. Opioid suppression of conditioned anticipatory brain responses to
449 breathlessness. *Neuroimage*, 150, pp.383–394. Available at:
450 <http://dx.doi.org/10.1016/j.neuroimage.2017.01.005>.

451 Hayen, A., Herigstad, M. & Pattinson, K.T.S., 2013. Understanding dyspnea as a complex individual
452 experience. *Maturitas*, 76(1), pp.45–50.

453 Haynes, J.-D., 2015. A Primer on Pattern-Based Approaches to fMRI: Principles, Pitfalls, and
454 Perspectives. *Neuron*, 87(2), pp.257–270.

455 Henderson, L.A., Rubin, T.K. & Macefield, V.G., 2010. Within-limb somatotopic representation of
456 acute muscle pain in the human contralateral dorsal posterior insula. *Human brain mapping*,
457 32(10), pp.1592–1601.

458 Herigstad, M. et al., 2011. Dyspnoea and the brain. *Respiratory medicine*, 105(6), pp.809–817.
459 Available at: <http://www.sciencedirect.com/science/article/pii/S0954611111000023>.

460 Herigstad, M. et al., 2017. Treating breathlessness via the brain: Mechanisms underpinning
461 improvements in breathlessness with pulmonary rehabilitation. *European Respiratory Journal*,
462 (50).

463 Holroyd, C.B. & Yeung, N., 2012. Motivation of extended behaviors by anterior cingulate cortex.
464 *Trends in Cognitive Sciences*, 16(2), pp.121–127.

465 Ito, S.I., 1998. Possible representation of somatic pain in the rat insular visceral sensory cortex: a
466 field potential study. *Neuroscience Letters*, 241(2-3), pp.171–174.

467 Kragel, P.A. et al., 2018. Generalizable representations of pain, cognitive control, and negative
468 emotion in medial frontal cortex. *Nature Neuroscience*, pp.1–15.

469 Krishnan, A. et al., 2016. Somatic and vicarious pain are represented by dissociable multivariate
470 brain patterns. *ELife*.

471 Kwong, K.K. et al., 1992. Dynamic magnetic resonance imaging of human brain activity during
472 primary sensory stimulation. *Proceedings of the National Academy of Sciences*, 89(12),
473 pp.5675–5679.

474 Lansing, R.W., Gracely, R.H. & Banzett, R.B., 2009. The multiple dimensions of dyspnea: Review
475 and hypotheses. *Respiratory physiology & neurobiology*, 167(1), pp.53–60. Available at:
476 <http://linkinghub.elsevier.com/retrieve/pii/S1569904808002000>.

477 Leupoldt, von, A. et al., 2009. Dyspnea and pain share emotion-related brain network. *Neuroimage*,
478 48(1), pp.200–206.

479 Liang, M. et al., 2013. Primary sensory cortices contain distinguishable spatial patterns of activity for
480 each sense. *Nature Communications*, 4, pp.1–10.

481 Lindquist, M.A. et al., 2017. Group-regularized individual prediction: theory and application to pain.
482 *Neuroimage*, 145(Part B), pp.274–287.

483 López-Solà, M. et al., 2019. Brain mechanisms of social touch-induced analgesia in females. *Pain*,
484 160(9), pp.2072–2085.

485 López-Solà, M. et al., 2017. Towards a neurophysiological signature for fibromyalgia. *Pain*, 158(1),
486 pp.34–47.

487 Ma, Y. et al., 2016. Serotonin transporter polymorphism alters citalopram effects on human pain
488 responses to physical pain. *Neuroimage*, 135(C), pp.186–196.

489 Mano, H. et al., 2018. Classification and characterisation of brain network changes in chronic back
490 pain: A multicenter study. *Wellcome Open Research*, 3, pp.19–24.

491 Marlow, L.L. et al., 2019. Breathlessness and the brain: the role of expectation. *Current Opinion in
492 Supportive and Palliative Care*, 13(3), pp.200–210.

493 Marquand, A. et al., 2010. Quantitative prediction of subjective pain intensity from whole-brain
494 fMRI data using Gaussian processes. *Neuroimage*, 49(3), pp.2178–2189.

495 Miyawaki, Y. et al., 2008. Visual Image Reconstruction from Human Brain Activity using a
496 Combination of Multiscale Local Image Decoders. *Neuron*, 60(5), pp.915–929.

497 Noesselt, T. et al., 2007. Audiovisual Temporal Correspondence Modulates Human Multisensory
498 Superior Temporal Sulcus Plus Primary Sensory Cortices. *Journal of Neuroscience*, 27(42),
499 pp.11431–11441.

500 Ohara, S. & Lenz, F.A., 2003. Medial Lateral Extent of Thermal and Pain Sensations Evoked By
501 Microstimulation in Somatic Sensory Nuclei of Human Thalamus. *Journal of Neurophysiology*,
502 90(4), pp.2367–2377.

503 Parshall, M.B. et al., 2012. An Official American Thoracic Society Statement: Update on the
504 Mechanisms, Assessment, and Management of Dyspnea. *American journal of respiratory and
505 critical care medicine*, 185(4), pp.435–452.

506 Ploner, M. et al., 1999. Parallel activation of primary and secondary somatosensory cortices in
507 human pain processing. *Journal of Neurophysiology*, 81(6), pp.3100–3104.

508 Reddan, M.C., Lindquist, M.A. & Wager, T.D., 2017. Effect Size Estimation in Neuroimaging.
509 *JAMA Psychiatry*, 74(3), pp.207–2.

510 Rosa, M.J. & Seymour, B., 2014. Decoding the matrix: Benefits and limitations of applying machine
511 learning algorithms to pain neuroimaging. *Pain*, 155(5), pp.864–867.

512 Segerdahl, A.R. et al., 2015. The dorsal posterior insula subserves a fundamental role in human pain.
513 *Nature Neuroscience*.

514 Seth, A.K., 2013. Interoceptive inference, emotion, and the embodied self. *Trends in Cognitive
515 Sciences*, 17(11), pp.565–573.

516 Singer, T. et al., 2004. Empathy for pain involves the affective but not sensory components of pain.
517 *science.scienmag.org*

518 .

519 Singer, T., Critchley, H.D. & Preuschoff, K., 2009. A common role of insula in feelings, empathy
520 and uncertainty. *Trends in Cognitive Sciences*, 13(8), pp.334–340.

521 Stephan, K.E. et al., 2016. Allostatic Self-efficacy: A Metacognitive Theory of Dyshomeostasis-
522 Induced Fatigue and Depression. *Frontiers in human neuroscience*, 10, pp.49–27.

523 Ung, H. et al., 2012. Multivariate Classification of Structural MRI Data Detects Chronic Low Back
524 Pain. *Cerebral Cortex*, 24(4), pp.1037–1044.

525 Van den Bergh, O. et al., 2017. Symptoms and the body: Taking the inferential leap. *Neuroscience &*
526 *Biobehavioral Reviews*, 74(Part A), pp.185–203. Available at:
527 <http://dx.doi.org/10.1016/j.neubiorev.2017.01.015>.

528 van der Miesen, M.M., Lindquist, M.A. & Wager, T.D., 2019. Neuroimaging-based biomarkers for
529 pain. *PAIN Reports*, 4(4), pp.e751–18.

530 Wager, T.D. et al., 2013. An fMRI-Based Neurologic Signature of Physical Pain. *New England*
531 *Journal of Medicine*, 368(15), pp.1388–1397.

532 Wiech, K., Ploner, M. & Tracey, I., 2008. Neurocognitive aspects of pain perception. *Trends in*
533 *Cognitive Sciences*, 12(8), pp.306–313.

534 Woo, C.-W. & Wager, T.D., 2016. What reliability can and cannot tell us about pain report and pain
535 neuroimaging. *Pain*, 157(3), pp.511–513.

536 Woo, C.-W. et al., 2015. Distinct Brain Systems Mediate the Effects of Nociceptive Input and Self-
537 Regulation on Pain M. Posner, ed. *PLoS Biology*, 13(1), pp.e1002036–14.

538 Woo, C.-W. et al., 2014. Separate neural representations for physical pain and social rejection.
539 *Nature Communications*, pp.1–12.

540 Woo, C.-W., Chang, L.J., et al., 2017. Building better biomarkers: brain models in translational
541 neuroimaging. *Nature Neuroscience*, 20(3), pp.365–377.

542 Woo, C.-W., Schmidt, L., et al., 2017. Quantifying cerebral contributions to pain beyond
543 nociception. *Nature Communications*, 8, pp.1–14.

544 Zunhammer, M., Bingel, U. & Wager, T.D., 2018. Placebo Effects on the Neurologic Pain Signature.
545 *JAMA Neurology*, 75(11), pp.1321–10.

546

547

581 **Supplementary Table 1:** NPS subregion analyses for 7 Tesla data contrasts of interest. Positive regions above the dotted
 582 line, negative regions below.
 583

<i>Anticipation</i>	<i>NPS</i>	<i>Error</i>	<i>t statistic</i>	<i>p value</i>	<i>Cohen's D</i>
Vermis	-0.074	0.133	-0.553	0.583	-0.087
Right Insula	6.993	1.813	3.857	<0.001	0.610
Right primary visual cortex	-2.435	1.352	-1.801	0.079	-0.285
Right thalamus	-0.091	0.263	-3.444	0.732	-0.054
Left insula	1.652	0.541	3.056	0.004	0.483
Right dorsal posterior insula	-0.527	0.282	-1.868	0.069	-0.295
Right secondary sensory cortex	0.817	0.613	1.332	0.191	0.211
Dorsal anterior cingulate cortex	2.534	1.599	1.585	0.121	0.251
Right lateral occipital cortex	1.717	0.574	2.994	0.005	0.473
Left lateral occipital cortex	1.572	0.753	2.087	0.043	0.330
Right posterior lateral occipital cortex	1.873	1.512	1.239	0.223	0.200
Pregenual anterior cingulate cortex	0.703	0.408	1.723	0.093	0.272
Left superior temporal sulcus	0.362	0.702	0.516	0.609	0.082
Right inferior parietal lobule	2.696	0.695	3.877	<0.001	0.613
Posterior cingulate cortex	0.070	0.433	0.163	0.872	0.026
<i>Breathlessness</i>	<i>NPS</i>	<i>Error</i>	<i>t statistic</i>	<i>p value</i>	<i>Cohen's D</i>
Vermis	0.392	0.125	3.145	0.003	0.497
Right Insula	9.087	1.986	4.576	<0.001	0.724
Right primary visual cortex	-0.520	1.233	-0.422	0.675	-0.067
Right thalamus	0.764	0.217	3.528	0.001	0.558
Left insula	2.557	0.530	4.824	<0.001	0.763
Right dorsal posterior insula	0.368	0.302	1.218	0.231	0.193
Right secondary sensory cortex	2.462	0.657	3.746	0.001	0.592
Dorsal anterior cingulate cortex	4.696	1.949	2.409	0.021	0.381
Right lateral occipital cortex	0.008	0.565	0.015	0.989	0.002
Left lateral occipital cortex	0.209	0.677	0.309	0.759	0.049
Right posterior lateral occipital cortex	-0.338	1.470	-0.230	0.819	-0.036
Pregenual anterior cingulate cortex	-0.023	0.409	-0.057	0.955	-0.009
Left superior temporal sulcus	-1.129	0.642	-1.758	0.087	-0.278
Right inferior parietal lobule	1.596	0.603	2.646	0.012	0.418
Posterior cingulate cortex	-0.319	0.404	-0.790	0.435	-0.125
<i>Finger opposition</i>	<i>NPS</i>	<i>Error</i>	<i>t statistic</i>	<i>p value</i>	<i>Cohen's D</i>
Vermis	0.804	0.144	5.582	<0.001	0.883
Right Insula	13.083	1.464	8.936	<0.001	1.413
Right primary visual cortex	9.634	0.727	13.242	<0.001	2.094
Right thalamus	0.693	0.146	4.754	<0.001	0.752
Left insula	4.063	0.426	9.548	<0.001	1.510
Right dorsal posterior insula	0.250	0.226	1.109	0.274	0.175
Right secondary sensory cortex	1.406	0.610	2.305	0.027	0.365
Dorsal anterior cingulate cortex	10.500	1.377	7.623	<0.001	1.205
Right lateral occipital cortex	-1.830	0.536	-3.412	0.002	-0.539
Left lateral occipital cortex	-4.492	0.484	-9.275	<0.001	-1.467
Right posterior lateral occipital cortex	-3.520	0.711	-4.951	<0.001	-0.783
Pregenual anterior cingulate cortex	0.569	0.291	1.956	0.058	0.309
Left superior temporal sulcus	-0.894	0.685	-1.305	0.200	-0.206
Right inferior parietal lobule	0.722	0.550	1.312	0.197	0.207
Posterior cingulate cortex	-0.311	0.282	-1.103	0.277	-0.174

Supplementary Table 2: NPS subregion analyses for 3 Tesla data contrasts of interest. Positive regions above the dotted line, negative regions below.

<i>Anticipation (saline)</i>	<i>NPS</i>	<i>Error</i>	<i>t statistic</i>	<i>p value</i>	<i>Cohen's D</i>
Vermis	-0.056	0.206	-0.274	0.788	-0.063
Right Insula	3.290	2.638	1.247	0.229	0.286
Right primary visual cortex	-3.703	1.575	-2.352	0.031	-0.540
Right thalamus	-0.186	0.366	-0.509	0.617	-0.117
Left insula	0.681	0.778	0.875	0.394	0.201
Right dorsal posterior insula	-1.304	0.452	-2.885	0.010	-0.662
Right secondary sensory cortex	0.265	0.806	0.329	0.746	0.075
Dorsal anterior cingulate cortex	1.122	3.667	0.306	0.763	0.070
Right lateral occipital cortex	0.053	0.593	0.089	0.930	0.020
Left lateral occipital cortex	1.502	1.280	1.174	0.257	0.269
Right posterior lateral occipital cortex	1.149	1.872	0.614	0.547	0.141
Pregenual anterior cingulate cortex	0.336	1.117	0.301	0.767	0.069
Left superior temporal sulcus	2.358	1.348	1.749	0.098	0.401
Right inferior parietal lobule	0.707	1.006	0.703	0.492	0.161
Posterior cingulate cortex	-0.840	0.569	-1.475	0.158	-0.338
<i>Anticipation (remifentanil)</i>	<i>NPS</i>	<i>Error</i>	<i>t statistic</i>	<i>p value</i>	<i>Cohen's D</i>
Vermis	0.269	0.175	1.540	0.141	0.353
Right Insula	4.008	1.576	2.544	0.020	0.584
Right primary visual cortex	-3.096	1.135	-2.728	0.014	-0.626
Right thalamus	0.350	0.211	1.656	0.115	0.380
Left insula	1.212	0.729	1.662	0.114	0.381
Right dorsal posterior insula	-0.368	0.387	-0.949	0.355	-0.218
Right secondary sensory cortex	-0.484	0.715	-0.677	0.507	-0.155
Dorsal anterior cingulate cortex	2.013	2.063	0.976	0.342	0.224
Right lateral occipital cortex	0.432	0.570	0.758	0.459	0.174
Left lateral occipital cortex	2.340	1.323	1.769	0.094	0.406
Right posterior lateral occipital cortex	2.891	1.162	2.487	0.023	0.571
Pregenual anterior cingulate cortex	-0.630	0.680	-0.926	0.367	-0.213
Left superior temporal sulcus	2.036	0.803	2.536	0.021	0.582
Right inferior parietal lobule	0.511	0.816	0.626	0.539	0.144
Posterior cingulate cortex	-0.108	0.389	-0.278	0.784	-0.064
<i>Saline > Remi Anticipation</i>	<i>NPS</i>	<i>Error</i>	<i>t statistic</i>	<i>p value</i>	<i>Cohen's D</i>
Vermis	-0.326	0.293	-1.111	0.282	-0.255
Right Insula	-0.719	3.200	-0.225	0.825	-0.052
Right primary visual cortex	-0.607	1.630	-0.373	0.714	-0.085
Right thalamus	-0.536	0.426	-1.260	0.225	-0.289
Left insula	-0.530	1.205	-0.440	0.666	-0.101
Right dorsal posterior insula	-0.936	0.674	-1.389	0.183	-0.319
Right secondary sensory cortex	0.749	1.126	0.665	0.515	0.153
Dorsal anterior cingulate cortex	-0.891	4.544	-0.196	0.847	-0.045
Right lateral occipital cortex	-0.379	0.893	-0.425	0.676	-0.098
Left lateral occipital cortex	-0.838	1.590	-0.527	0.605	-0.121
Right posterior lateral occipital cortex	-1.742	1.976	-0.882	0.390	-0.202
Pregenual anterior cingulate cortex	0.966	1.477	0.654	0.522	0.150
Left superior temporal sulcus	0.322	1.566	0.206	0.840	0.047

Right inferior parietal lobule	0.196	0.882	0.222	0.827	0.051
Posterior cingulate cortex	-0.732	0.663	-1.104	0.285	-0.253
<i>Breathlessness (saline)</i>	<i>NPS</i>	<i>Error</i>	<i>t statistic</i>	<i>p value</i>	<i>Cohen's D</i>
Vermis	0.089	0.088	1.018	0.323	0.234
Right Insula	5.807	1.285	4.519	<0.001	1.037
Right primary visual cortex	0.821	1.043	0.787	0.442	0.181
Right thalamus	0.475	0.101	4.684	<0.001	1.075
Left insula	1.497	0.368	4.066	<0.001	0.933
Right dorsal posterior insula	0.018	0.150	0.122	0.904	0.028
Right secondary sensory cortex	1.667	0.360	4.636	<0.001	1.064
Dorsal anterior cingulate cortex	3.424	1.350	2.537	0.021	0.582
Right lateral occipital cortex	-0.603	0.573	-1.052	0.308	-0.241
Left lateral occipital cortex	-0.700	0.612	-1.145	0.268	-0.263
Right posterior lateral occipital cortex	0.536	0.962	0.558	0.584	0.128
Pregenual anterior cingulate cortex	0.882	0.271	3.254	0.005	0.746
Left superior temporal sulcus	-0.595	0.583	-1.021	0.322	-0.234
Right inferior parietal lobule	0.166	0.409	0.406	0.690	0.093
Posterior cingulate cortex	0.035	0.290	0.122	0.904	0.028
<i>Breathlessness (remifentanil)</i>	<i>NPS</i>	<i>Error</i>	<i>t statistic</i>	<i>p value</i>	<i>Cohen's D</i>
Vermis	0.005	0.102	0.050	0.961	0.011
Right Insula	0.993	1.196	0.831	0.417	0.191
Right primary visual cortex	0.409	0.970	0.422	0.678	0.097
Right thalamus	0.026	0.095	0.269	0.791	0.062
Left insula	-0.008	0.317	-0.024	0.981	-0.006
Right dorsal posterior insula	-0.453	0.174	-2.613	0.018	-0.599
Right secondary sensory cortex	0.521	0.455	1.145	0.267	0.263
Dorsal anterior cingulate cortex	0.245	1.253	0.195	0.847	0.045
Right lateral occipital cortex	-0.193	0.395	-0.489	0.631	-0.112
Left lateral occipital cortex	-0.668	0.598	-1.118	0.278	-0.256
Right posterior lateral occipital cortex	1.306	0.915	1.428	0.171	0.328
Pregenual anterior cingulate cortex	0.756	0.246	3.075	0.007	0.705
Left superior temporal sulcus	0.281	0.578	0.486	0.633	0.112
Right inferior parietal lobule	0.444	0.443	1.002	0.330	0.230
Posterior cingulate cortex	0.236	0.237	0.996	0.332	0.227
<i>Saline > Remi breathlessness</i>	<i>NPS</i>	<i>Error</i>	<i>t statistic</i>	<i>p value</i>	<i>Cohen's D</i>
Vermis	0.084	0.116	0.724	0.479	0.166
Right Insula	4.813	1.731	2.781	0.013	0.638
Right primary visual cortex	0.412	1.107	0.372	0.714	0.085
Right thalamus	0.449	0.142	3.164	0.006	0.726
Left insula	1.505	0.494	3.049	0.007	0.699
Right dorsal posterior insula	0.472	0.165	2.854	0.011	0.655
Right secondary sensory cortex	1.146	0.431	2.657	0.017	0.610
Dorsal anterior cingulate cortex	3.179	1.640	0.938	0.069	0.445
Right lateral occipital cortex	-0.409	0.430	-0.953	0.354	-0.219
Left lateral occipital cortex	-0.032	0.647	-0.050	0.961	-0.011
Right posterior lateral occipital cortex	-0.770	0.870	-0.885	0.388	-0.203
Pregenual anterior cingulate cortex	0.126	0.376	0.336	0.741	0.077
Left superior temporal sulcus	-0.876	0.642	-1.363	0.191	-0.313
Right inferior parietal lobule	-0.277	0.426	-0.651	0.524	-0.149
Posterior cingulate cortex	-0.200	0.296	-0.676	0.508	-0.155

593

594

595 **Supplementary Figures**

596

597

598

599

600

601

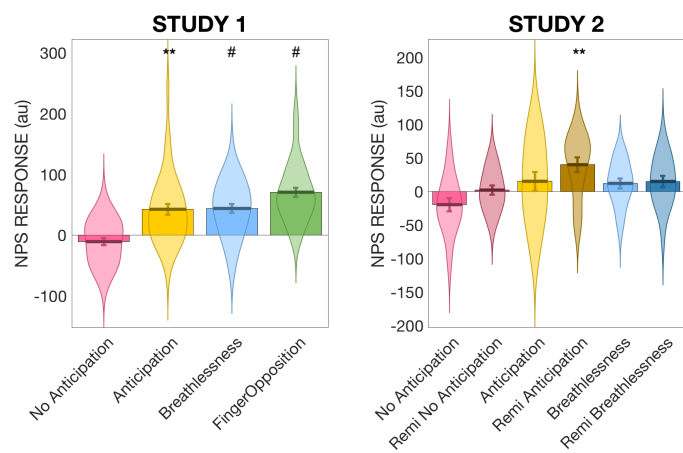
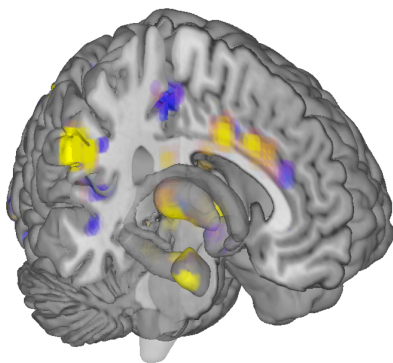
602

603

604

605

606



607

Supplementary Figure 1. Overall NPS activity in all conditions for the two datasets. Left: Three-dimensional representation of some of the core regions of the NPS. ** Significantly different from zero at $p < 0.01$; # Significantly different from zero at $q < 0.05$ (FDR corrected).

611

612

613

614

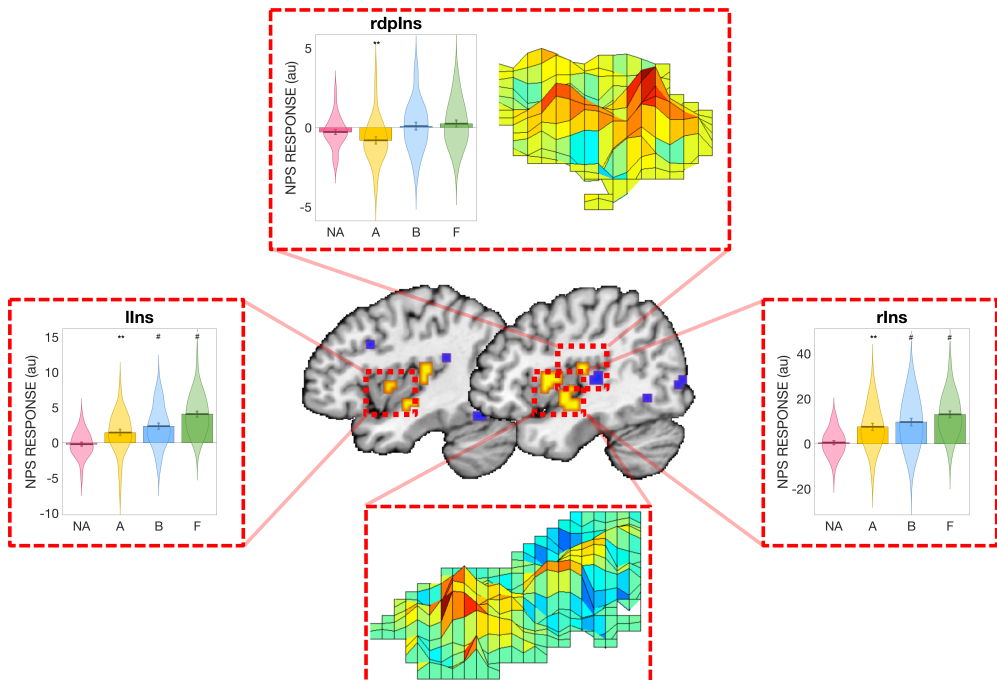
615

616

617

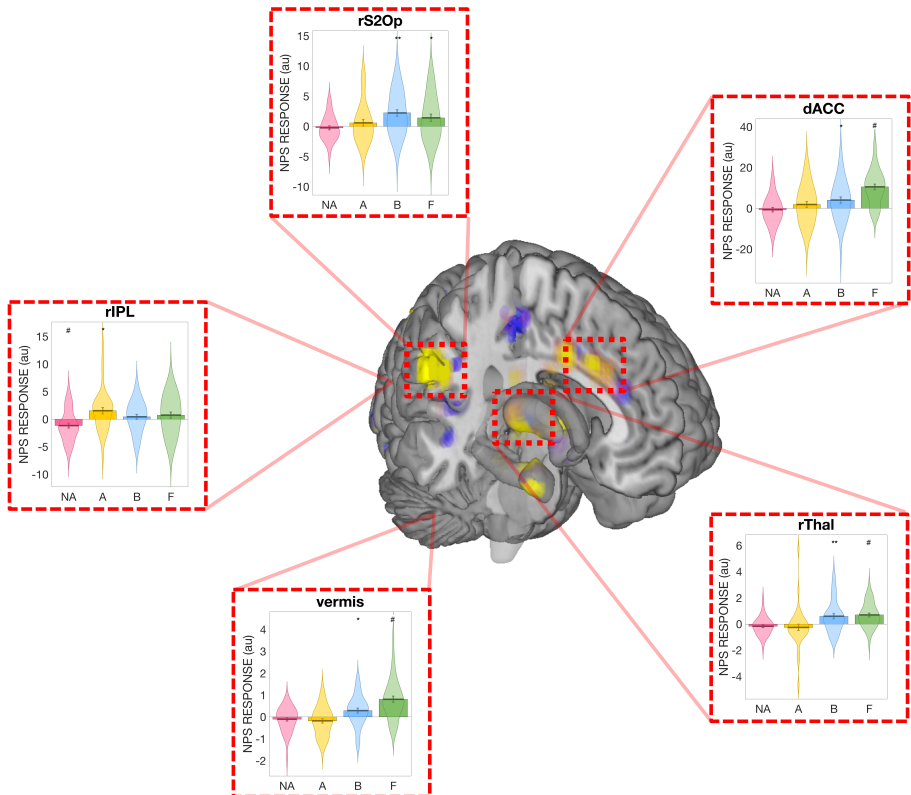
618

619
620
621
622
623
624
625
626



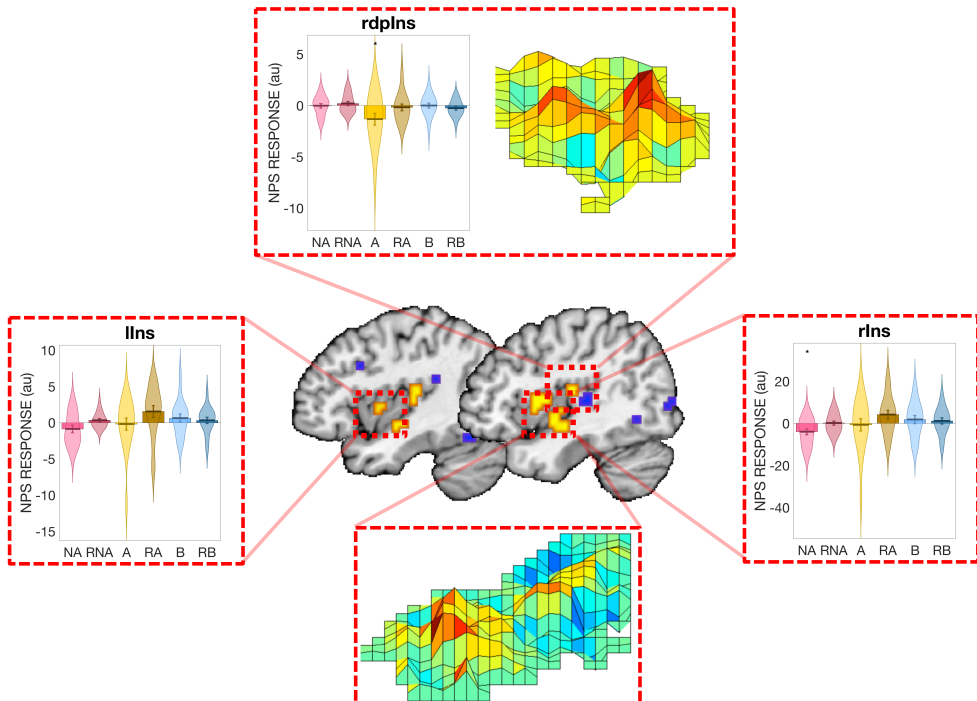
627
628 **Supplementary Figure 2.** Regional NPS activity in the insula for the no-anticipation, anticipation, breathlessness and finger
629 opposition conditions from Study 1. Robust statistical activity is observed in the bilateral insula (labelled lIns and rIns) for
630 all except the no-anticipation condition, while no significant positive activity is observed in the right dorsal posterior insula
631 (rdpIns). Abbreviations: NA, No anticipation; A, Anticipation; B, Breathlessness; F, Finger opposition. ** Significantly
632 different from zero at $p < 0.01$; # Significantly different from zero at $q < 0.05$ (FDR corrected).
633
634

635
636
637
638
639
640



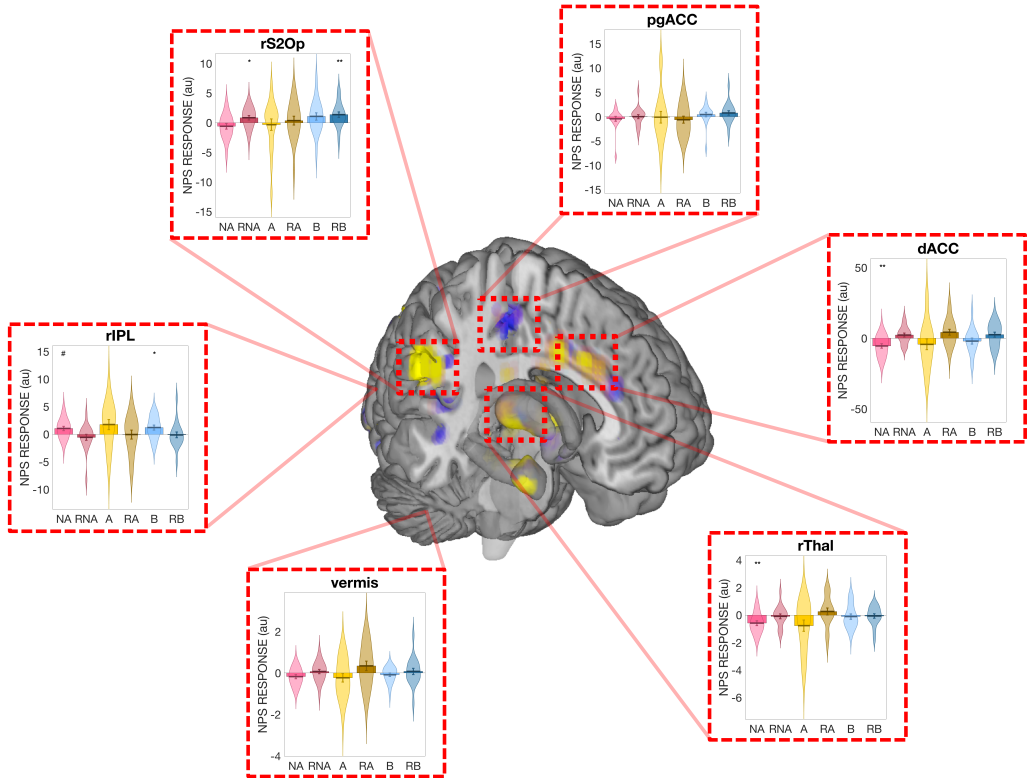
641
642 **Supplementary Figure 3.** Regional NPS activity subregions of the NPS for the no-anticipation, anticipation, breathlessness
643 and finger opposition conditions from Study 1. Abbreviations: dACC, dorsal anterior cingulate cortex; rThal, right
644 thalamus; rS2Op, right secondary somatosensory cortex / operculum; rIPL, right inferior parietal lobule; NA, No
645 anticipation; A, Anticipation; B, Breathlessness; F, Finger opposition. * Significantly different from zero at $p < 0.05$; **
646 Significantly different from zero at $p < 0.01$; # Significantly different from zero at $q < 0.05$ (FDR corrected).
647
648

649
650
651
652
653
654
655
656



657
658 **Supplementary Figure 4.** Regional NPS activity in the insula for the no-anticipation, anticipation and breathlessness
659 conditions during both saline and remifentanil administration from Study 2. Abbreviations: rIns, right insula; lIns, left
660 insula; rdpIns, right dorsal posterior insula; NA, No anticipation; A, Anticipation (saline); RA, Remifentanil anticipation;
661 B, Breathlessness (saline); RB, Remifentanil breathlessness. ** Significantly different from zero at $p < 0.01$; # Significantly
662 different from zero at $q < 0.05$ (FDR corrected).
663

664
665
666
667
668
669
670
671



672
673 **Supplementary Figure 5.** Regional NPS activity subregions of the NPS for the no-anticipation, anticipation and
674 breathlessness conditions during both saline and remifentanil administration from Study 2. Abbreviations: dACC, dorsal
675 anterior cingulate cortex; pgACC, pregenual anterior cingulate cortex; rThal right thalamus; rS2Op, right secondary
676 somatosensory cortex / operculum; rIPL, right inferior parietal lobule; A, Anticipation contrast (saline); RA, Remifentanil
677 anticipation contrast; B, Breathlessness contrast (saline); RB, Remifentanil breathlessness contrast. * Significantly
678 different from zero at $p < 0.05$; ** Significantly different from zero at $p < 0.01$; # Significantly different from zero at $q <$
679 0.05 (FDR corrected).
680